Statistical Associating Fluid Theory of Homopolymers and Block Copolymers in Compressible Solutions: Polystyrene, Polybutadiene, Polyisoprene, Polystyrene-*block*-Polybutadiene, and Polystyrene-*block*-Polyisoprene in Propane†

Sugata Pikatan Tan, W. Winoto, and Maciej Radosz*

Soft Materials Laboratory, Department of Chemical & Petroleum Engineering, University of Wyoming, Laramie, Wyoming 82071-3295

Received: May 14, 2007; In Final Form: August 17, 2007

Polystyrene, polybutadiene, polyisoprene, and their diblock copolymers can form compressible homogeneous solutions in propane that separate upon decompression into a solvent-rich phase and a polymer-rich phase. If the styrene block is large enough, the diblock copolymers can also form a pressure-tunable micellar nanophase that exists below the micellization pressure but above the cloud-point pressure. The onset of micellization and cloud-point transitions can be realistically estimated within a statistical associating fluid theory (SAFT1) framework using universal SAFT1 parameters characteristic of the segment volumes and segment energies, except for the segment−segment interaction energy between the two blocks, which requires an adjustment to account for different types of cloud-point and micellar transitions.

Introduction

Block copolymer molecules can be designed to consist of two or more blocks of segments with distinctly different affinities to a solvent. In dilute solutions, if the solvent is selective enough for the different blocks that belong to the same block-copolymer molecules, these molecules can form spherical micelles,[1] which consist of a solvent-phobic core and solvent-philic corona. This capacity to self-assemble into micelles has led to extensive research on and numerous practical applications of block copolymers.[2,3] Nearly all literature data are on their dilute solutions in relatively incompressible liquid solvents.[4] Colina et al.[5] qualitatively estimated cloud points and critical micelle densities from the osmotic pressure in supercritical carbon dioxide using a statistical associating fluid theory (SAFT)[6] with averaging rules for the block copolymer. Another example of using SAFT for approximating amphiphilic mixtures is a sphere-and-bond formalism,[7] which however is not applicable to real systems yet.

In a recent work,[8] both bulk cloud-point pressures and micelle-formation pressures were measured for polystyrene-*block*-polyisoprene in propane. That work suggested that the isothermal micelle-formation pressure curves, consistent with the isobaric micelle-formation temperature curves, are reminiscent of the corresponding cloud-point curves. The goal of this work is to take additional experimental data, for polystyrene-*block*-polybutadiene and polystyrene-*block*-polyisoprene in propane, to understand the underlying thermodynamic forces within the mean-field framework of statistical associating fluid theory (SAFT1)[9] that builds on a copolymer SAFT concept originally proposed by Banaszak et al.[10] to account explicitly for heteronuclear chains using segment fractions and bond fractions. Banaszak's approach was confirmed with simulation data, for example, for pure hard-chain copolymers[11] and Lennard-Jones copolymers.[12] Its numerous applications have been reviewed by Spyriouni and Economou.[13]

In order to extend SAFT1 to real block-copolymer solutions, one could hypothesize that micelle formation is a kind of nanophase equilibrium involving a bulk solvent-rich phase and a copolymer-rich micellar phase, as the micelles, including their cores,[1] contain solvent molecules. This hypothesis is different from a so-called pseudophase model of micellar aggregation,[14] where the copolymer clusters, not the copolymer molecules in the micellar phase, are in the state of equilibrium with the unimers, that is, the individual copolymer molecules, in the solvent-rich phase. While these models can account for the onset of micelle formation, they cannot explicitly account for the micelle structure, for example, for its size and shape, which is the province of other theories, such as density functional theory.[15]

Experimental Section

The cloud-point experiments, using transmitted-light intensity, and the micelle formation and decomposition experiments, using scattered-light intensity, are carried out in a variable volume titanium cell equipped with sapphire windows and optical fibers that connect it with the detector and lasers (wavelengths of 632.8 nm and 488 nm, respectively). This experimental setup, tested at pressures up to 2,000 bar, is shown in Figure 1. Test results and a detailed description were reported previously.[8]

The homopolymers and diblock copolymers used in this work were purchased from Polymer Source, Inc., except for PS-*b*-PBD (9−23), which was generously provided by Professor Jimmy Mays (University of Tennessee at Knoxville). Their properties are given in Table 1.

PBD and PiP homopolymers and their blocks are of the 1,4-addition type, as shown in Figure 2.

SAFT1 Model and Its Parameters. The residual Helmholtz energy of these polymers and of their compressible solutions is approximated with a copolymer version of SAFT referred to as SAFT1.[9] As it is common for the SAFT models, this approximation separates different types of interactions among the

† Part of the "Keith E. Gubbins Festschrift".

* Corresponding author. E-mail: radosz@uwyo.edu.

10.1021/jp073701s CCC: $37.00
Published on Web 10/06/2007 PAGE EST: 6.7

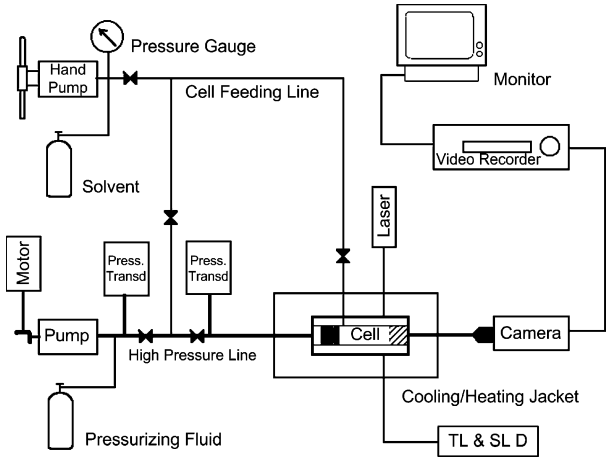

Figure 1. High-pressure transmitted- and scattered-light intensity cell.

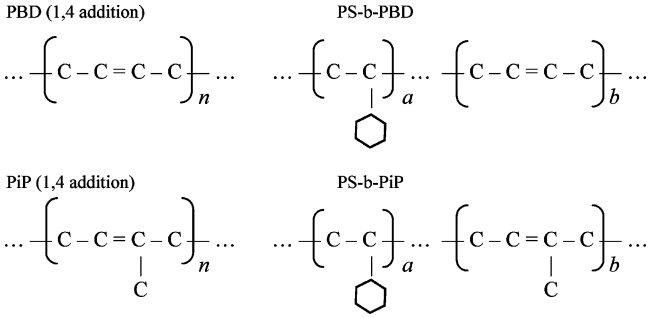

Figure 2. Repeating units.

segments of like and unlike molecules. Since the polymers used in this work are nonassociating, the dimensionless residual Helmholtz energy can be written as

$$\tilde{a}^{\mathrm{res}} = \tilde{a}^{\mathrm{hs}} + \tilde{a}^{\mathrm{disp}} + \tilde{a}^{\mathrm{chain}} \tag{1}$$

The superscripts mean the residual, hard-sphere, dispersion, and chain terms, respectively. Detailed derivations and definitions are documented elsewhere.[9] The advantage of SAFT1 is that it explicitly accounts for different types of segments in a single molecule and hence explicitly accounts for composition of heterosegmented molecules, such as random and blocky copolymers, as proposed by Banaszak et al.[10] Even though this copolymer SAFT approach does not explicitly account for the exact position of each segment in the molecule, it can implicitly but quantitatively account for the copolymer blockiness through bond fractions, as described below.

As SAFT1 uses square-well potential for the dispersive energy, it requires four parameters to characterize segment α in real molecules: the segment number m_α, the segment volume v_α^{00}, the segment energy u_α^0, and the square-well width parameter λ_α.

Homopolymers. The PBD (1,4 addition) homopolymer has two alternating chemical groups, $-CH_2-CH_2-$, the same as in polyethylene, and $-CH=CH-$, as shown in Figure 2. These two chemical groups are approximated with SAFT1 segments for ethane and ethylene and labeled α and β, respectively. As it has been done before, the SAFT1 parameters can be estimated from simple but reliable molecular weight correlations. For example, for segment α, the SAFT1 parameters are estimated as follows:[9]

$$m_\alpha = 0.023763\, M_\alpha + 0.618823 \tag{2a}$$

$$m_\alpha v_\alpha^{00} = 0.599110\, M_\alpha + 4.640260 \tag{2b}$$

$$m_\alpha u_\alpha^0/k = 6.702340\, M_\alpha + 19.67793 \tag{2c}$$

$$m_\alpha \lambda_\alpha = 0.039308\, M_\alpha + 1.104297 \tag{2d}$$

The molecular weight of segments α can be calculated as a fraction of the polymer number-averaged molecular weight M_n:

$$M_\alpha = (28/54) M_n \tag{3}$$

The fraction in eq 3 reflects the PBD repeating unit structure in Figure 2, the molecular weight of which is 54 (4 carbon atoms and 6 hydrogen atoms). Segment α consists of 2 carbon atoms and 4 hydrogen atoms, while segment β is the remaining part with the double bond.

In SAFT1, the total segment number of the whole polymer molecule is obtained from eq 2a by replacing M_α with M_n. Therefore, for PBD, the number of segments β is

$$m_\beta = 0.023763 M_\beta \tag{4}$$

$$M_\beta = (26/54) M_n \tag{5}$$

Since segments α and β are similar in size, we use eq 2b to calculate the segment volume of β from

$$m_\beta v_\beta^{00} = 0.599110 M_\beta + 4.640260 \tag{6}$$

The segment energy of segment β, which is different from that of segment α, is adjusted to match the experimental cloud-point data; the u_β^0 and λ_β correlations are presented in Results and Discussion.

Having estimated the segment parameters, one needs to estimate the fraction of each segment,

$$\gamma_\alpha = m_\alpha/(m_\alpha + m_\beta) \tag{7a}$$

$$\gamma_\beta = m_\beta/(m_\alpha + m_\beta) \tag{7b}$$

and the fractions of the like- and the unlike-segment bonds. Even though the chemical groups $-CH_2-CH_2-$ and $-CH=CH-$ alternate along the backbone, the corresponding SAFT1 segments α and β do not strictly alternate and hence they lead to small fractions of like-segment bonds, $B_{\alpha\alpha}$ and $B_{\beta\beta}$.

TABLE 1: Polymers Used in This Work

polymer	abbreviation	M_n[a] (× 1000 g/mol)	polydispersity index[b]
polybutadiene	PBD	58; 18; 8.8; 5.3; 1.75	1.05; 1.04; 1.04; 1.04; 1.1
polyisoprene	PiP	76.5; 30; 10.1; 3	1.07; 1.04; 1.04; 1.06
polystyrene-block-polybutadiene	PS-*b*-PBD	9.4−9; 5.4−5.35; 9.1−65; 28.4−13.6	1.03; 1.03; 1.04; 1.03
polystyrene-block-polyisoprene	PS-*b*-PiP	9−23; 11.5−10.5	1.01; 1.04

[a] M_n = number-averaged molecular weight. [b] Polydispersity index = M_w/M_n; M_w = weight-averaged molecular weight

TABLE 2: SAFT1 Segment Parameters

segment	m	v^{00} [cc/mol]	u^0/k [K]	λ
α	eq 2a	eq 2b/eq 2a	eq 2c/eq 2a	eq 2d/eq 2a
β	eq 4	eq 6/eq 4	eq 16a/eq 4	eq 16b/eq 4
C	eq 10	15.039[b]	eq 17a	1.7827[b]
P[a]	[x]	19.958	248.660	1.6614
S[b]	1.667	18.492	193.223	1.6914

[a] From ref 17; [b] From ref 9; [x]: the total segment number for PS is the same as that estimated from the polyethylene correlation. Hence, the branch segment number is the difference between its total segment number [x] and its backbone segment number.

All of these bond fractions, like and unlike, are calculated as follows:

$$B_{\alpha\alpha} = \frac{m_\alpha}{(4/3)}((4/3) - 1)\frac{1}{m_\alpha + m_\beta - 1} \tag{8a}$$

$$B_{\beta\beta} = \frac{m_\beta}{1.4578}(1.4578 - 1)\frac{1}{m_\alpha + m_\beta - 1} \tag{8b}$$

$$B_{\alpha\beta} = 1 - B_{\alpha\alpha} - B_{\beta\beta} \tag{8c}$$

where the denominator $m_\alpha + m_\beta - 1$ is the total number of bonds in each molecule, 4/3 is the segment number of ethane,[9] and 1.4758 is the segment number of ethylene, derived in this work, as usual, from its vapor pressure and saturated liquid volume.[16] Therefore, each ethane segment contributes $(4/3 - 1) = 1/3$ of αα bond, and each ethylene segment contributes $(1.4578 - 1) = 0.4578$ of $\beta\beta$ bond.

In each repeating PiP unit, we have an additional methyl branch (segment C), which leads to 3 segments for PIP: α and β, as in PBD, and C. The parameters v^{00} and λ for C are taken to be the same as those for methane. Its energy u^0 is derived from the experimental cloud-point data and hence will be presented in Results and Discussion.

The number of PiP segments per molecule is calculated from eqs 2a and 4 as follows:

$$M_\alpha = (28/68)M_n \tag{9a}$$

$$M_\beta = (25/68)M_n \tag{9b}$$

This is because the PP repeating unit shown in Figure 1 has a molecular weight of 68. Then the segment number of type C is simply:

$$m_C = 0.023763\, M_C \tag{10}$$

$$M_C = M_n - M_\alpha - M_\beta = (15/68)M_n \tag{11}$$

The corresponding segment fractions for segments α and β are calculated from eq 7a,b with an expression for C as follows:

$$\gamma_C = 1 - \gamma_\alpha - \gamma_\beta \tag{12}$$

While eq 8a and eq 8b are still valid for the like-segment bond fractions, the unlike-segment bond fractions must be derived from the repeating unit structure; there are twice as many $\alpha\beta$ bonds as βC bonds:

$$B_{\alpha\beta} = 2\, B_{\beta C} = (2/3)(1 - B_{\alpha\alpha} - B_{\beta\beta}) \tag{13}$$

A similar approach was found[17] to work for the PS molecules. PS has two types of segments, that is, α and P (the phenyl group). Segment P was approximated with benzene, except for the segment energy, which was derived from cloud-point pressures for PS + propane solutions, along with a binary P-propane parameter. These parameters are tabulated in Tables 2 and 3.

TABLE 3: Binary Interaction Parameters

binary parameters	temperature dependence (T in [K])	reference
$k_{\alpha S}$	$0.02939 - 6.0 \times 10^{-5}\, T$	18
$k_{\beta S}$	$0.01026 + 5.2143 \times 10^{-5}\, T$	this work, eq 16c
k_{CS}	$-0.0037 - 5.27 \times 10^{-5}\, T$	this work, eq 17b
k_{PS}	$0.04697 - 3.9 \times 10^{-5}\, T$	17
$k_{\beta P}$	0.033	this work, eq 18

Equations 2a−d are still valid for segments α, but now with

$$M_\alpha = (27/104)M_n \tag{14}$$

where 104 is the molecular weight of the PS repeating unit. While the segment fractions can be estimated from eq 7a,b, but with subscript P instead of β, the bond fractions have new formulations:

$$B_{\alpha\alpha} = \frac{m_\alpha - 1}{m_\alpha + m_P - 1} \tag{15a}$$

$$B_{PP} = \frac{m_P}{1.954}\frac{1}{m_\alpha + m_P - 1} \tag{15b}$$

where 1.954 is the SAFT1 segment number for benzene.[17] The unlike-segment bond fraction, $B_{\alpha P}$, is calculated from eq 8c with subscript P instead of β.

The binary interaction energies between polymer segments and solvent segments require parameters commonly obtained from cloud-point data for polymer solutions[17,18] and given in Table 3. The binary parameters obtained in this work are also presented in Results and Discussion. The binary parameters for the like segments, αα and $\beta\beta$, are set equal to zero.

Block Copolymers. Each copolymer molecule consists of two blocks, A and B. The molecular weight of each block is determined experimentally. The segment parameters are analogous to those for the corresponding homopolymers, that is, there are four sets of segment parameters for PS-*b*-PBD (two sets for the PS block and two sets for the PBD block) and five sets for PS-*b*-PiP (two sets for the PS block and three sets for the PiP block). The segment and bond fractions are calculated with respect to the whole molecule.

Since the copolymers studied in this work are relatively large, the single block−block bond (A−B bond) is crucial in keeping the two blocks together, but it contributes very little to the SAFT1 chain term. As the copolymer is a species with properties significantly different from those of the individual blocks, this A−B bond contribution to the chain term alone, therefore, is not enough to differentiate the copolymer from a corresponding mixture of homopolymers A and B, and specifically it is not enough to account for the reduced dispersive energy of interaction between the segments that belong to different blocks, compared with the corresponding homopolymers. One way to account for this is to reduce the dispersive energy of interaction between the segments that belong to different blocks, β and P in this case, relative to the segment−solvent interaction energy, using a binary parameter, $k_{\beta P}$, as follows:

$$u_{\beta P} = \sqrt{u_\beta u_P}(1 - k_{\beta P}) \tag{16}$$

This $k_{\beta P}$ parameter is derived from one set of copolymer cloud-point data, as illustrated in Results and Discussion, and used without readjustment for all other cloud-point data.

TABLE 4: Cloud-Point Pressures of PBD in Propane (Figure 3)

$M_n = 58000$		$M_n = 18000$		$M_n = 8800$		$M_n = 5300$		$M_n = 1750$	
T [K]	P [bar]	T [K]	P [bar]	T [K]	P [bar]	T [K]	P [bar]	T [K]	P [bar]
293.4	872.1	293.1	495.1	293.1	267.9	293.1	98.5	353.0	34.9
313.3	753.6	303.2	470.2	303.2	265.2	303.2	112.7	373.0	67.1
353.2	641.3	313.2	453.1	313.2	266.3	313.2	126.3	393.2	94.9
393.2	598.1	333.2	435.3	333.3	275.7	333.1	153.6	413.1	116.8
433.0	585.3	353.1	427.9	353.2	289.3	353.2	180.4	433.0	135.7
452.9	579.7	373.2	428.8	373.2	304.3	373.2	205.7		
		393.3	434.1	393.1	320.5	393.0	229.4		
		413.2	440.9	413.1	335.3	413.1	250.0		
		433.2	447.6	433.2	348.8	433.2	267.2		

TABLE 5: Cloud-Point Pressures of PiP in Propane (Figure 4)

$M_n = 76500$		$M_n = 30000$		$M_n = 10100$		$M_n = 3000$	
T [K]	P [bar]	T [K]	P [bar]	T [K]	P [bar]	T [K]	P [bar]
293.5	366.4	293.3	252.2	293.2	95.6	333.3	56.0
313.4	365.1	313.2	266.4	313.1	130	353.9	89.3
353.5	384	354.5	304.3	353.3	192.8	373.3	121.2
393.7	412.4	393.9	339.6	373.5	218.6	393.4	146.8
433.3	436.2	433.6	372.3	393.4	246.1	413.3	169.2
		453.4	382.1	433.5	286.7	433.2	181.4
				453.0	301.7	453.1	192.5

TABLE 6: Cloud-Point Pressures of PS-*b*-PBD (Figures 5−7) and PS-*b*-PiP (Figure 8) in Propane

Figure 5		Figure 6		Figure 7		Figure 8	
T [K]	P [bar]	T [K]	P [bar]	T [K]	P [bar]	T [K]	P [bar]
293.1	1097.8	303.2	637.7	303.2	987.0	293.2	489.7
303.1	1008.4	313.0	563.8	313.2	868.5	313.2	410.6
313.2	932.3	333.3	480.9	333.1	737.3	333.2	381.8
333.2	762.0	353.6	441.1	353.2	678.9	353.2	376.2
353.2	642.1	392.8	417.2	373.2	644.1	373.0	378.3
373.4	582.4	433.2	419.1	393.2	622.6	393.2	382.6
393.1	547.4	451.6	432.4	413.2	608.8	413.2	378.8
413.1	529.2			433.2	599.3	433.0	383.6
433.2	516.9			453.2	575.8	453.0	384.8
453.2	507.4						

Micellization Hypothesis. The experimental cloud-point data for the homopolymers suggest that propane is a stronger solvent for PBD and PiP (it requires lower pressure to dissolve them) and a weaker solvent for PS (it requires higher pressure to dissolve it). Therefore, propane is expected to be a selective solvent for the corresponding diblocks. If the difference in its affinity to the two blocks is large enough (if it is selective enough), propane can lead to micelle formation. Since each micelle, with a solvent-philic corona and a solvent-phobic core, is known to contain some solvent,[1] we approximate its state with a state of phase equilibrium, where the micelles form a solvent-lean but copolymer-rich nanophase dispersed and coexisting in equilibrium with a solvent-rich copolymer-lean continuous phase.

In such a nanophase equilibrium approximation, the transition from a disordered homogeneous solution to a micellar solution implies that the individual blocks stay together in pairs that form the copolymer molecules, but retain their original affinities to the solvent. In other words, we need to enforce the block pair stoichiometry, but allow the blocks to interact with each other in the presence of the solvent as if they did in an unbonded homopolymer state. This means that there is no need to adjust the block−block dispersive interaction energy relative to the block−solvent dispersive interaction energy (as we do for the bulk cloud-point transitions), and hence the $k_{\beta P}$ parameter will be set equal to zero.

A practical advantage of such a nanophase equilibrium approximation is that one can use the well-established bulk phase equilibrium calculation procedures to describe both the nanophase phase transitions (when $k_{\beta P} = 0$) and the bulk cloud points (when $k_{\beta P} \neq 0$).

Results and Discussion

Homopolymer in Propane. The experimentally determined properties and SAFT1 parameters for PS in propane solutions used in this work are the same as those reported previously.[17] The properties and SAFT1 parameters for the other homopolymers solutions are determined in this work. The experimental data taken in this work are tabulated in Tables 4−7. Figure 3 shows the experimental and calculated cloud points of PBD in propane, upon fitting of u_β^0, λ_β, and the binary interaction parameter between segment β in PBD and solvent S ($k_{\beta S}$), with the average absolute deviation (AAD) of about 5 bar. This fit can be represented by simple empirical expressions as follows:

$$m_\beta u_\beta^{\,0}/k = 5.75 M_\beta - 914.720 \quad (17a)$$

$$m_\beta \lambda_\beta = 0.03994 M_\beta + 0.6045 \quad (17b)$$

$$k_{\beta S} = 0.01026 + 5.2143 \times 10^{-5}\, T\,[\text{in K}] \quad (17c)$$

These expressions will be used in all other calculations in this work, without further readjustment.

TABLE 7: Cloud-Point Pressures and Micellization of PS-*b*-PBD (Figure 9) and PS-*b*-PiP (Figure 10) in Propane (the Latter Measured in Ref 8)

Figure 9 cloud points		Figure 9 micellization		Figure 10 cloud points		Figure 10 micellization	
T [K]	P [bar]	T [K]	P [bar]	T [K]	P [bar]	T [K]	P [bar]
293.4	1080.9	358.0	1556.7	293.1	451.2	333.2	1002.0
303.2	981.8	363.7	1420.1	313.1	438.0	328.0	1002.1
313.2	922.2	373.5	1225.2	333.2	441.8	393.8	551.4
322.9	893.3	373.4	1242.9	353.1	451.8	395.0	555.8
332.9	867.5	383.3	1106.3	373.1	471.6	323.3	1165.6
353.3	812.6	393.3	1017.4	413.0	502.5	323.2	1092.5
373.2	780.2	403.2	943.5	453.3	504.6	348.1	787.3
393.2	755.8	413.1	894.3			348.1	767.5
413.3	739.0	423.0	850.2			372.7	680.3
433.1	728.2	433.1	890.0			372.9	639.3
452.9	724.1					372.9	616.0
						373.0	639.6
						373.0	611.4
						333.0	948.1
						333.0	901.5

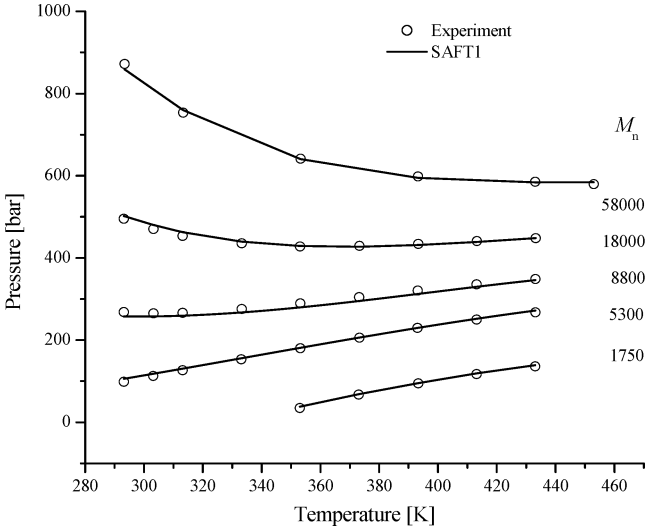

Figure 3. Cloud points of PBD (0.5 wt %) in propane.

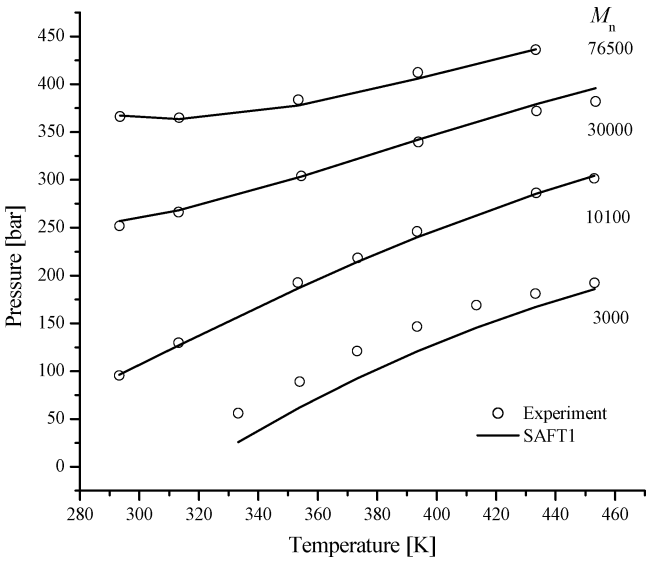

Figure 4. Cloud points of PiP (0.5 wt %) in propane.

Figure 4 shows the experimental and calculated cloud points of PiP in propane, upon fitting of u_C^0 and the binary interaction parameter between segment C in PiP and solvent segment S (k_{CS}), with the average absolute deviation (AAD) of about 9 bar. This fit can be represented by simple empirical expressions as follows:

$$u_C^0/k = 146.9126 \text{ [K]} \tag{18a}$$

$$k_{CS} = -0.0037 - 5.27 \times 10^{-5}\, T \text{ [in K]} \tag{18b}$$

Diblock Copolymer in Propane. Not all diblock copolymers used in this work exhibit micellization. If the PS block is not large enough relative to the other block, micelles cannot be formed. This is because the difference of the block−solvent affinities, and hence the solvent selectivity, is not sufficient to form micelles.

Such diblock systems that do not exhibit micellization are a convenient starting point for a SAFT1 analysis. Figure 5 shows experimental and calculated pressure−temperature cloud points for a PS-*b*-PBD diblock as well as the corresponding block-forming homopolymers. Their molecular weights are shown in parentheses. As expected, the cloud-point pressures of the diblock fall between those of the corresponding homopolymers.

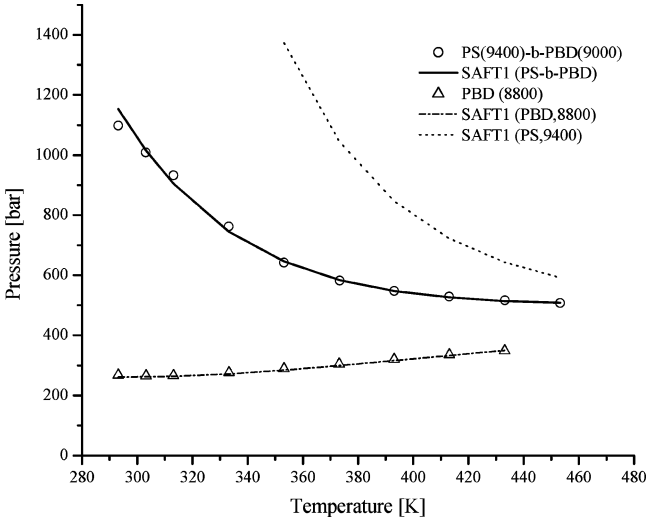

Figure 5. Cloud points of PS, PBD, and PS-*b*-PBD (0.5 wt %) in propane.

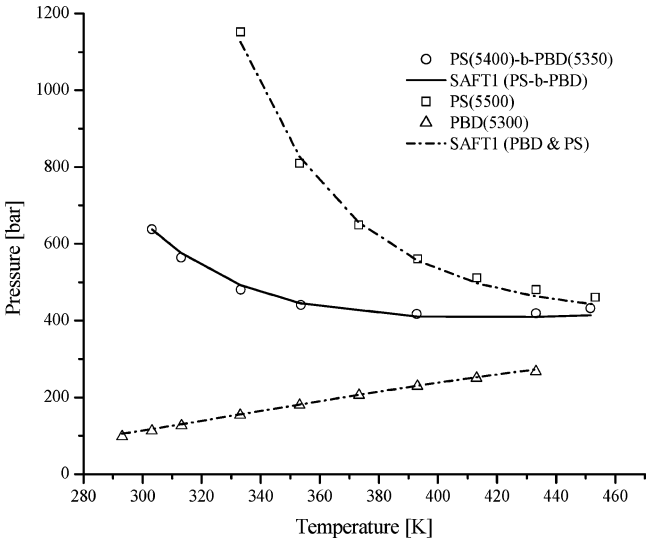

Figure 6. Cloud points of PS, PBD, and symmetric PS-*b*-PBD (0.5 wt %) in propane.

The PBD cloud points are calculated using the parameters obtained in this work, while the PS cloud points are calculated using the parameters obtained by Tan et al.[17] For the diblock, the SAFT1 parameters are taken from the previous correlations, without further readjustment, except for a binary parameter that adjusts the interaction energy between segments β in PBD and segments P in PS ($k_{\beta P}$), which is derived from the experimental cloud-point data with AAD of 15 bar. The value for this parameter happens to be a constant:

$$k_{\beta P} = 0.033 \tag{19}$$

In order to test its physical significance, this parameter is used to predict the properties of other PS-*b*-PBD systems, without further readjustment. The results are presented in Figure 6 for PS-*b*-PBD with a molecular weight different from that in Figure 5 and in Figure 7 for a PS-*b*-PBD that is strongly asymmetric. In both cases, the SAFT1 predictions turned to capture the experimental curves realistically.

For an asymmetric PS-*b*-PiP system shown in Figure 8, with a relatively large PiP block, as expected, no micellization is observed. The cloud-point predictions shown in Figure 8, without any fitting, are less accurate than those for the PS-*b*-

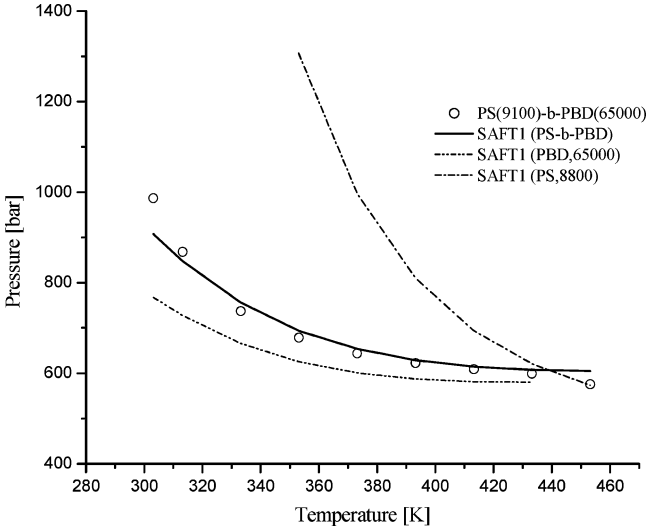

Figure 7. Cloud points of PS, PBD, and asymmetric PS-*b*-PBD (0.5 wt %) in propane.

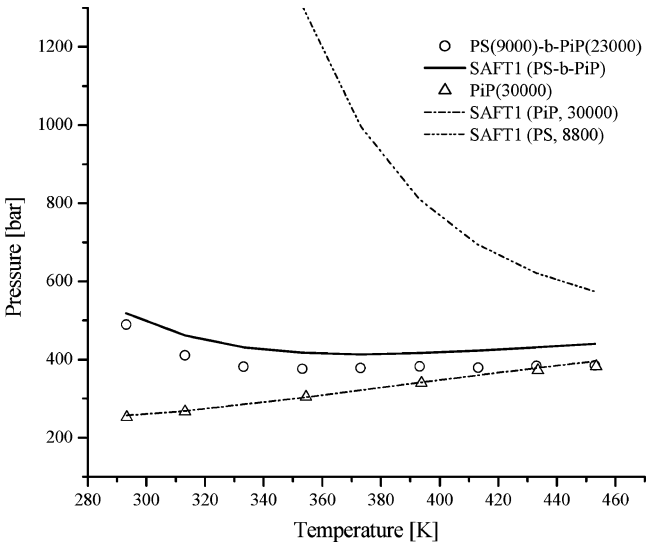

Figure 8. Cloud points of PS-*b*-PiP (0.5 wt %) + propane and SAFT1 prediction.

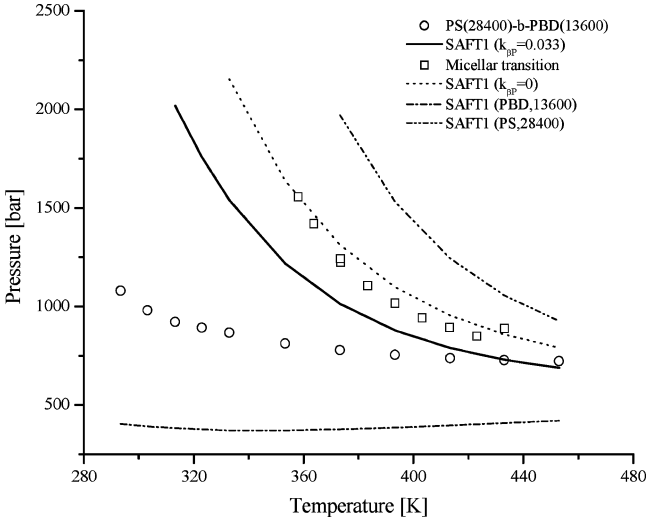

Figure 9. Cloud points and micellization of PS-*b*-PBD (0.5 wt %) in propane.

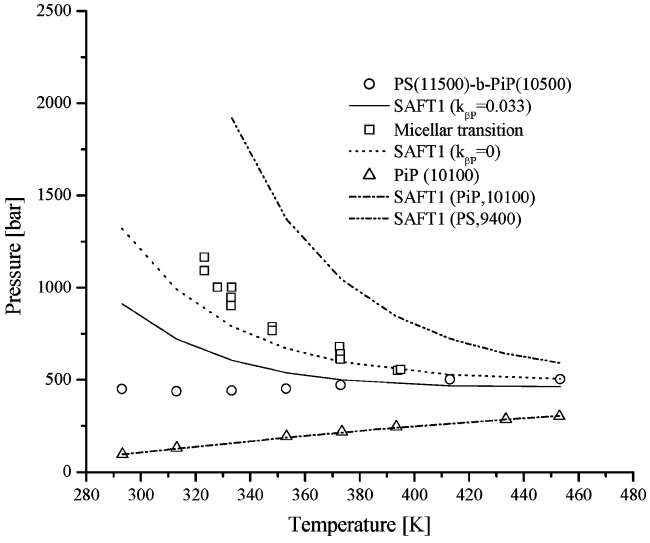

Figure 10. Cloud points and micellization of PS-*b*-PiP (0.5 wt %) in propane (experimental data are taken from our previous work[8]).

PBD systems, but they are realistic, including the proximity of the diblock curve to that of the large PiP curve.

When the PS block is large enough to form micelles, the measured diblock cloud-point pressures, shown with open circles in Figures 9 and 10, are overestimated by SAFT1. This is shown with a solid curve predicted with the same value of the binary interaction parameter $k_{\beta P} = 0.033$ as that used to predict the onset of the bulk two-phase separation starting from a homogeneous solution. This is because the experimental cloud points in Figures 9 and 10 have a different physical meaning, namely, they represent the onset of a bulk two-phase separation starting from a micellar solution instead. The bulk-phase separation pressure is lower for the micellar solution compared with that of the homogeneous solution because of a corona-stabilizing effect. In other words, propane is a better solvent (requires lower pressures) for the micelles than it is for the corresponding homogeneous solution. This effect could be captured by revisiting the $k_{\beta P}$ parameter to match the measured micellar-solution cloud-point pressures, but this correction is not a trivial and requires more work.

As expected, the homogeneous-solution predictions, with $k_{\beta P} = 0.033$, become realistic above the micelle decomposition temperatures, where the cloud points means a conventional transition from a disordered homogeneous solution to a bulk two-phase system.

Finally, in order to verify the micellization hypothesis, namely, that the onset of micelle formation can be approximated as a nanophase separation (a transition from a homogeneous solution to a micellar solution), we predict it using the same SAFT1 parameters as those used to calculate all of the other cloud-point transitions, except for $k_{\beta P}$ that is set equal to zero. The calculated results, shown as dotted curves in Figures 9 and 10, capture the experimental micellization points, shown as squares in Figures 9 and 10. While such mean-field calculations cannot shed light on the micelle structure, they can be used to estimate the onset of micellization, which is an important technology issue in designing processes to make micellar nanoparticles, such as those used for drug and gene delivery.

Conclusion

Polystyrene, polybutadiene, polyisoprene, and their diblock copolymers can form compressible homogeneous solutions in propane that separate upon decompression into a solvent-rich phase and a polymer-rich phase. If the styrene block is large

enough, the diblock copolymers can also form a pressure-tunable micellar nanophase that exists below the micellization pressure but above the cloud-point pressure. The onset of micellization and cloud-point transitions can be realistically estimated within a statistical associating fluid theory (SAFT1) framework using universal SAFT1 parameters characteristic of the segment volumes and segment energies, except for the segment−segment interaction energy between the two blocks, which requires an adjustment to account for different types of cloud-point and micellar transitions.

Acknowledgment. This work is funded by an NSF Grant CTS-0244388. M.R. gratefully acknowledges the collaboration with Professor Keith E. Gubbins and his associates at Cornell University, Walter G. Chapman and George Jackson, initiated two decades ago in an effort to understand associating molecules. While the funding incentive at that time was to understand asphaltene aggregation, it was the polymer technology that inspired early SAFT applications.

Glossary

Polymers

PBD	Polybutadiene
PiP	Polyisoprene
PS	Polystyrene
PS-*b*-PBD	Polystyrene-*block*-Polybutadiene
PS-*b*-PiP	Polystyrene-*block*-Polyisoprene

Segment-Type Subscripts

α	segment type of "—C—C—" in PBD, PS, and PiP
β	segment type of "—C═C—" in PBD and PiP
C	segment type of methyl branches in PiP
P	segment type of phenyl branches in PS
S	segment type of the solvent

SAFT1 Parameters

m	segment number
u^0	segment energy
v^{00}	segment volume
λ	square-well width parameter

Others

$\tilde{a}$	dimensionless Helmholtz energy
AAD	average absolute deviation

$$AAD = \sqrt{\frac{\sum (P_{calc} - P_{exp})^2}{n}}$$

P_{calc} = calculated pressure; P_{exp} = measured pressure; n = the number of experimental points

B	the fraction of a bond type in the molecule
γ	the fraction of a segment type in the molecule
k	Boltzmann constant
k_{ij}	binary interaction parameter between segment i and segment j
M_n	number-averaged molecular weight
T	absolute temperature [K]

References and Notes

(1) Quintana, J. R.; Villacampa, M.; Katime, I. A. *Macromolecules* **1993**, *26*, 601.
(2) Legge, N. R.; Holden, G.; Schroeder, H. E. *Thermoplastic Elastomers*; Hanser Publishers: Munich, 1987.
(3) Hamley, I. W. *The Physics of Block Copolymers;* Oxford University Press: New York, 1998.
(4) Loh, W. In *Encyclopedia of Surface and Colloid Science*; Hubbard, A., Ed.; Marcel Dekker, Inc.: New York, 2002, p 802.
(5) Colina, C. M.; Hall, C. K.; Gubbins, K. E. *Fluid Phase Equilib*. **2002**, *553*, 194−197.
(6) Huang, S. H.; Radosz, M. *Ind. Eng. Chem. Res*. **1991**, *30*, 1994.
(7) Kuespert, D. R.; Donohue, M. D. *J. Phys. Chem*. **1995**, *99*, 4805.
(8) Winoto, W.; Adidharma, H.; Shen, Y.; Radosz, M. *Macromolecules* **2006**, *39*, 8140.
(9) Adidharma, H.; Radosz, M. *Ind. Eng. Chem. Res*. **1998**, *37*, 4453.
(10) Banaszak, M.; Chen, C. K.; Radosz, M. *Macromolecules* **1996**, *29*, 6481.
(11) Shukla, K. P.; Chapman, W. G. *Mol. Phys*. **1997**, *91*, 1075.
(12) Banaszak, M.; Radosz, M. *Fluid Phase Equilib.* **2002**, *193*, 179.
(13) Spyriouni, T.; Economou, I. G. *Polymer* **2005**, *46*, 10772.
(14) Nagarajan, R.; Ruckenstein, E. In *Equation of State for Fluids and Fluid Mixtures*; Sengers, J. V., Kayser, R. F., Peters, C. J., White, H. J., Eds.; IUPAC: Amsterdam, 2000; p 597.
(15) Uneyama, T.; Doi, M. *Macromolecules* **2005**, *38*, 5817.
(16) Smukala, J.; Span, R.; Wagner, W. *J. Phys. Chem. Res. Data* **2000**, *29*, 1053.
(17) Tan, S. P.; Meng, D.; Plancher, H.; Adidharma, H.; Radosz, M. *Fluid Phase Equilib*. **2004**, *226*, 189.
(18) Chan, A.; Adidharma, H.; Radosz, M. *Ind. Eng. Chem. Res*. **2000**, *39*, 3069.